J. Phycol. **59,** 87–96 (2023)

DOI: 10.1111/jpy.13303

THE EFFECT OF CYTOSKELETON INHIBITORS ON COCCOLITH MORPHOLOGY IN *COCCOLITHUS BRAARUDII* AND *SCYPHOSPHAERA APSTEINII*[1]

Gerald Langer[2]

Marine Biological Association, The Laboratory, Citadel Hill, Plymouth PL1 2PB, UK

Ian Probert

Station Biologique de Roscoff, 29680 Roscoff, France

Madison B. Cox, Alison Taylor

Department of Biology and Marine Biology, University of North Carolina Wilmington, Wilmington, North Carolina, 28403-591, USA

Glenn M. Harper

Plymouth Electron Microscopy Centre, University of Plymouth, Plymouth PL4 8AA, UK

Colin Brownlee

Marine Biological Association, The Laboratory, Citadel Hill, Plymouth PL1 2PB, UK
School of Ocean and Earth Science, University of Southampton, Southampton SO14 3ZH, UK

and Glen Wheeler[2]

Marine Biological Association, The Laboratory, Citadel Hill, Plymouth PL1 2PB, UK

The calcite platelets of coccolithophores (Haptophyta), the coccoliths, are among the most elaborate biomineral structures. How these unicellular algae accomplish the complex morphogenesis of coccoliths is still largely unknown. It has long been proposed that the cytoskeleton plays a central role in shaping the growing coccoliths. Previous studies have indicated that disruption of the microtubule network led to defects in coccolith morphogenesis in *Emiliania huxleyi* and *Coccolithus braarudii*. Disruption of the actin network also led to defects in coccolith morphology in *E. huxleyi*, but its impact on coccolith morphology in *C. braarudii* was unclear, as coccolith secretion was largely inhibited under the conditions used. A more detailed examination of the role of actin and microtubule networks is therefore required to address the wider role of the cytoskeleton in coccolith morphogenesis. In this study, we have examined coccolith morphology in *C. braarudii* and *Scyphosphaera apsteinii* following treatment with the microtubule inhibitors vinblastine and colchicine (*S. apsteinii* only) and the actin inhibitor cytochalasin B. We found that all cytoskeleton inhibitors induced coccolith malformations, strongly suggesting that both microtubules and actin filaments are instrumental in morphogenesis. By demonstrating the requirement for the microtubule and actin networks in coccolith morphogenesis in diverse species, our results suggest that both of these cytoskeletal elements are likely to play conserved roles in defining coccolith morphology.

Key index words: **actin; calcification; coccolith; coccolithophore; cytoskeleton; microtubule**

***Abbreviations*: DCMU, 3-(3,4-dichlorophenyl)-1,1-dimethylurea; EGTA, ethylene glycol-bis(2-aminoethyl ether)-N,N,N′,N′-tetraacetic acid**

Coccolithophores, haptophyte algae, are among the most important pelagic calcite producers (Baumann et al. 2004, Poulton et al. 2007, Ziveri et al. 2007). The calcite platelets (coccoliths) that form the cell covering display an intricate morphology including elaborately shaped crystals in the diploid life cycle stage (Young et al. 1999). Although definitive evidence for the precise function of calcification in coccolithophores has been difficult to obtain, it is likely that assembly of coccoliths into a protective coccosphere is central to their function (Monteiro et al. 2016). For instance, it was shown that the interlocking coccosphere of *E. huxleyi* confers remarkable mechanical protection, and *C. braarudii* needs an intact coccosphere to divide (Jaya et al. 2016, Walker et al. 2018). The distinct,

[1]Received 14 June 2022. Accepted 20 September 2022.
[2]Author for correspondence: e-mails gerald.langer@cantab.net (G. L.); glw@mba.ac.uk (G. W.)
Editorial Responsibility: R. Wetherbee (Associate Editor)

normal morphology of the coccoliths is required for the correct formation of the coccosphere (Young 1994, Henriksen et al. 2003, Bown et al. 2004, Quintero-Torres et al. 2006, Jaya et al. 2016, Walker et al. 2018). Morphogenesis of coccoliths is therefore a central element of coccolithophore eco-physiology and evolution. Despite this prime position in coccolithophore biology, the morphogenesis of coccoliths is not well understood. Just over a decade ago, coccolith morphogenesis was still regarded as "the most enigmatic part of biomineralization" (Henriksen et al. 2004). Although some progress has been made in the last decade, this statement has lost little of its edge.

While Huxley (1868) initially regarded coccoliths as of inorganic origin, it is now clear that the morphologies of coccolith crystals are not to be found in inorganically precipitated calcite (Young et al. 1999, Aquilano et al. 2016). Calcification in coccolithophores occurs intracellularly, allowing precise control of the chemical conditions for the precipitation of calcium carbonate. The coccolith develops in a specialized intracellular compartment, the coccolith vesicle (Dixon 1900, Wilbur and Watabe 1963), where calcium carbonate crystals are nucleated onto an organic baseplate to produce small, initially rhombic crystals in precise crystallographic orientations. The calcite crystals then undergo carefully controlled growth to produce mature coccoliths with distinctive morphologies for each species. The mature coccoliths are subsequently secreted to the cell surface, where they are arranged to form the coccosphere. The cytoskeleton likely plays several important roles in coccolithogenesis, including controlling the exocytosis of the coccolith vesicle to the cell surface. Significant research interest has focused on the requirement for the cytoskeleton in shaping the morphology of the developing coccolith.

The coccolith vesicle adopts the shape of the growing coccolith (Outka and Williams 1971, Klaveness 1972, Westbroek et al. 1984, Probert et al. 2007, Kadan et al. 2021), which has led to the hypothesis that the coccolith vesicle acts as dynamic mold for the developing coccolith (Klaveness 1972, Young et al. 1999). This view includes a controlled force that shapes the coccolith vesicle. Based on transmission electron microscopy (TEM) examination of developing coccoliths, it was hypothesized that a fibrillar structure adjacent to the coccolith vesicle exerts this force (Klaveness 1972, 1976). This led to the idea that the fibrillar material, later equated with the cytoskeleton (Remak 1843, Freud 1882), is at the center of the coccolith shaping machinery (Westbroek et al. 1984, Didymus et al. 1994, Marsh 1994, 1999, Young et al. 1999, 2009, Marsh et al. 2002). Although this hypothesis is widely accepted, the supporting evidence from TEM analysis remains somewhat ambiguous (Klaveness 1972, 1976). This ambiguity was not eliminated by later TEM studies (Westbroek et al. 1984, Taylor et al. 2007). Recently, immunofluorescence microscopy has revealed a microtubule network in close contact with the coccolith vesicle in *Coccolithus braarudii* (Durak et al. 2017). This observation complements the earlier TEM studies and strongly supports the original dynamic mold hypothesis (Klaveness 1972, 1976).

The cytoskeleton is central to many aspects of cellular function. While many chemical inhibitors exist that disrupt the function of the microtubule and actin networks within the cell, their use to examine specific processes is complicated by their potential to interfere with other aspects of cell physiology. However, Langer et al. (2010) demonstrated that the application of microtubule and actin inhibitors to coccolithophores could be carefully titrated to partially disrupt cytoskeleton function without complete inhibition of cellular growth. Application of the microtubule inhibitor colchicine or the actin inhibitor cytochalasin B to the abundant bloom-forming species *Emiliania huxleyi* resulted in significant disruption of coccolith morphology. These malformations were not observed in other treatments that reduced growth rate (e.g., the photosynthesis inhibitor 3-(3,4-dichlorophenyl)-1,1-dimethylurea (DCMU)), leading to the conclusion that both actin and microtubules play a central role in controlling the morphology of the developing coccolith. These findings therefore provide experimental support for the dynamic mold hypothesis.

A subsequent study observed similar effects on coccolith morphology in *Coccolithus braarudii* using the microtubule inhibitor nocodazole (Durak et al. 2017). The effect of disrupting actin in *C. braarudii* was however different, as it led to a complete inhibition of coccolith production. Actin may therefore play a more general role in coccolith production in *C. braarudii*, such as the exocytosis of coccoliths or the initiation of coccolith formation, although this does not preclude an additional role in coccolith morphogenesis (Durak et al. 2017). Considering that both TEM and immunofluorescence imaging (Taylor et al. 2007, Durak et al. 2017) have so far only provided evidence for the involvement of microtubules in morphogenesis, evidence for the role of actin in coccolithogenesis remains limited.

It is important to note that the pharmacological agents used to disrupt the cytoskeleton in these studies have distinct modes of action (Table S1 in the Supporting Information; Langer et al. 2010, Durak et al. 2017). Moreover, Langer et al. (2010) examined coccolith morphology in *Emiliana huxleyi* cells grown in test conditions for several generations, whereas Durak et al. (2017) disrupted cytoskeletal networks in decalcified *Coccolithus braarudii* cells and then assessed their ability to recalcify. These methodological differences make it difficult to directly ascertain the wider requirement for actin in coccolith formation in coccolithophores.

We have therefore performed a detailed examination of the impact of cytoskeleton disruption on coccolith formation in two coccolithophore species. *Coccolithus braarudii* is a heavily calcified species that is abundant in temperate and sub-polar regions of the North Atlantic and contributes significantly to calcification in this regions (Daniels et al. 2016). To obtain a broader picture of the effects of cytoskeleton inhibitors on coccolith morphology, we have additionally examined *Scyphosphaera apsteinii*. This dimorphic species produces two distinct coccolith types, the disc-like muroliths and the large barrel-shaped lopadoliths (Drescher et al. 2012). Moreover, *S. apsteinii* is a member of the Zygodiscales and therefore occupies a distinct evolutionary lineage from *Emiliana huxleyi* (Isochrysidales) and *C. braarudii* (Coccolithales). We have treated *C. braarudii* and *S. apsteinii* with a range of inhibitors that act to disrupt actin and microtubule function within the cell. We show that both components of the cytoskeleton play an important role in coccolith morphogenesis in these species.

MATERIAL AND METHODS

Culture conditions. Clonal cultures of *Coccolithus braarudii* (strain PLY182g) and *Scyphosphaera apsteinii* (strain RCC1456) were grown in aged (3 months), sterile-filtered (Stericup-GP Sterile Vacuum Filtration System, 0.22 µm pore size, polyethersulfone membrane, Merck) natural surface seawater sampled in the English Channel off Plymouth, UK (station E1: 50°02.00' N, 4°22.00' W) enriched with 100 µM nitrate, 6.25 µM phosphate, 4 µM silicate, 0.005 µM H_2SeO_3, 0.00314 µM $NiCl_2$, and trace metals and vitamins as in f/2 medium (Guillard 1975). Strain RCC1456 was obtained from the Roscoff Culture Collection (http://www.sb-roscoff.fr/Phyto/RCC), and strain PLY182g from the Plymouth Culture Collection (https://www.mba.ac.uk/facilities/culture-collection#b7).

Cultures were grown under a 16:8 h light:dark cycle. Experiments were carried out at a light intensity of 50 µmol photons $\cdot$ m^{-2} $\cdot$ s^{-1} in temperature-controlled culture rooms. *Coccolithus braarudii* PLY182g was grown at 15°C, and *Scyphosphaera apsteinii* was grown at 18°C. Cells were grown in dilute batch cultures, ensuring a quasi-constant seawater carbonate system over the course of the experiment (Langer et al. 2013). Each data point is the mean value of triplicate culture experiments. Error bars represent SD.

For determination of cell density, samples were taken every other day (or less frequently, depending on growth rate) and counted immediately after sampling using a Sedgwick Rafter Counting Cell. Cell densities were plotted versus time, and growth rate (µ) was calculated from exponential regression using the natural logarithm.

Application of cytoskeleton inhibitors. Colchicine, vinblastine, and cytochalasin B were obtained from Sigma-Aldrich (Munich, Germany).

Vinblastine was dissolved in reverse osmosis water. The concentration of the stock solution was 1.1 mM. *Coccolithus braarudii* was treated with a final vinblastine concentration of 2 µM, and *Scyphosphaera apsteinii* with a final vinblastine concentration of 1.25 µM.

Colchicine was dissolved in culture medium. The concentration of the stock solution was 2.5 mM. *Scyphosphaera apsteinii* was treated with a final colchicine concentration of 20 µM.

Cytochalasin B stock solution (20.9 mM in DMSO) was obtained from Sigma-Aldrich (Munich, Germany). *Coccolithus braarudii* was treated with a final cytochalasin B concentration of 1.5 µM, and *Scyphosphaera apsteinii* with a final cytochalasin B concentration of 1 µM. Consequently, cells were exposed to a maximum DMSO concentration of 0.007 vol %. This DMSO concentration is harmless; it was shown that in *Emiliana huxleyi* 0.5 vol % DMSO has no effect on growth rate (Langer et al. 2010). In confirmation, *C. braarudii* and *S. apsteinii* grown in 0.01 vol % DMSO showed normal growth, and upon qualitative inspection by means of light microscopy, no notable increase in coccolith malformations.

All stock solutions were freshly prepared prior to the start of the experiments. Cells were exposed to cytoskeleton inhibitors for 25 d, after which samples were taken for analysis of coccolith morphology. We did not monitor any potential degradation of the inhibitor during the course of the experiment, although we assume that this was minimal due to the substantial effects on calcification that were observed. The prolonged incubation period ensured that the majority of coccoliths observed on the cells had been generated during the test period, rather than prior to the application of the inhibitor.

Decalcification of Coccolithus braarudii *cells.* To examine the impact of decalcification on coccolith morphology, two different treatments were applied, EGTA and low pH. To decalcify with EGTA, buffered (pH 8.2) calcium-free artificial seawater treatment containing 25 mM EGTA was added to cells for 30–45 min, followed by perfusion with fresh F/2 culture medium (Taylor and Brownlee 2003). To decalcify with low pH, 40 µL of 1.0 M HCl was added to a 5 mL aliquot of culture to lower pH to around 2.5, immediately followed by the addition of 40 µL 1.0 M NaOH by gentle mixing to restore pH back to ~8. This process took no more than ~5 min, after which low pH-decalcified cells were plated out and observed at the same time points as above. Cells were plated onto coverslip petri dishes and observed at 0, 4, 8, and 24 h post-decalcification using an Olympus IX71 inverted microscope equipped with a digital color camera (Infinity 1, Lumenera Corp. Ontario, Canada).

SEM analysis of coccolith morphology. Samples for SEM analysis were filtered on polycarbonate filters (0.8 µm pore-size), dried in a drying cabinet at 50°C for 24 h, then sputter-coated with gold–palladium using an Emitech K550 sputter coater at Plymouth Electron Microscopy Centre (PEMC). Imaging was performed with both Jeol JSM-6610LV and Jeol JSM-7001F at PEMC. The following categories were used to describe coccolith morphology. (1) *Coccolithus braarudii*: normal, malformation type R, minor malformation, major malformation, rhomb-like malformation. For reference images see Figure 1. A preliminary analysis showed that the percentage of incomplete coccoliths was less than 1% in all samples. Therefore, incomplete coccoliths were not accurately quantified in the final analysis. (2) *Scyphosphaera apsteinii*: normal, malformation type R, malformation type S, malformation type T. For reference images and a full description of each morphological category see Figure 5. An average of ~350 coccoliths was analyzed per sample (Langer and Benner 2009). The methodology of coccolith categorization and counting employed here is well established and yields robust and unbiased results (Langer et al. 2006, Langer and Benner 2009, Langer and Bode 2011, Bach et al. 2012, Langer et al. 2012).

The percentage of intact coccospheres was also analyzed in the samples used for coccolith morphology. Intact coccospheres were defined as coccospheres that did not collapse during preparation for SEM imaging. Coccolith

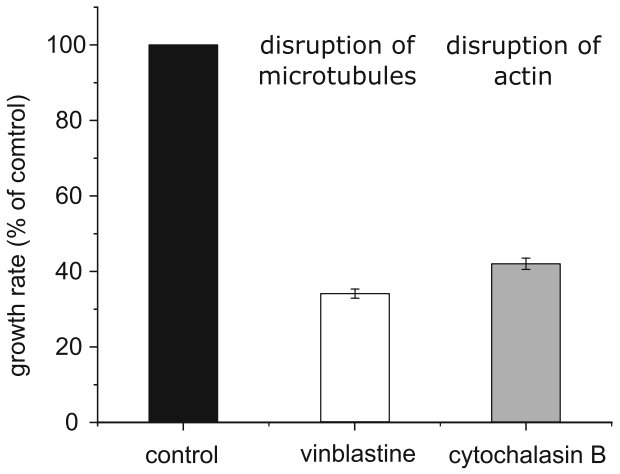

FIG. 1. Effects of cytoskeletal inhibitors on growth of *Coccolithus braarudii*. A Growth rate of *C. braarudii* following treatment with 1.25 μM vinblastine or 2 μM cytochalasin B. Growth is shown relative to control (untreated) cultures as the vinblastine and cytochalasin B treatments had separate controls (specific growth rates of the controls ranged from 0.5–0.6 · d^{-1}). n = 3 cultures for each treatment. Error bars represent SD.

malformations impair the ability of the coccoliths to interlock and reduce the structural rigidity of the coccosphere, making it more likely to collapse. Note that coccospheres that collapse during preparation for SEM imaging could still represent a complete coccosphere around the cell in culture. An average of ~300 coccospheres was analyzed per sample. Data presented in the figures are averages of triplicate cultures; error bars represent SD. The percentage of intact coccospheres was only analyzed in *Coccolithus braarudii* because *Scyphosphaera apsteinii* coccoliths do not interlock and show high percentages of collapsed coccospheres in all samples.

RESULTS

Effects of cytoskeletal inhibitors on Coccolithus braarudii. To examine the impacts of disrupting the cytoskeleton on coccolith formation in *Coccolithus braarudii*, we treated cells with the microtubule inhibitor vinblastine and the actin inhibitor cytochalasin B. As the cytoskeleton is essential for cell division and many other cellular processes, a total disruption of cytoskeletal function would prevent cell growth or secretion of coccoliths. We therefore performed a series of pre-experiments to determine inhibitor concentrations that allow the cells to continue to grow at a reduced growth rate, indicating that the inhibitor disrupts the cytoskeleton to some extent but does not completely impair secretion or cell division.

Growth of *Coccolithus braarudii* cells in 2 μM cytochalasin B to disrupt actin networks resulted in a 58% reduction in growth rate (Fig. 1). Application of 1.25 μM vinblastine to disrupt microtubule function reduced growth by 66%. Scanning electron microscopy (SEM) was then used to examine coccolith morphology in these cultures. Despite the similar reduction in growth rate, the effects of the two different inhibitors on coccolith morphology were markedly different. In general, the effects of cytochalasin B were more severe than the ones of vinblastine. In particular, the percentage of major malformations (0.0% in the control) rose to 7.3 ± 0.5% under the influence of vinblastine but to 17.7 ± 1.1% under cytochalasin B treatment (n = 3, ± SD; Fig. 2). The level of minor malformations did not differ between the two inhibitors (Table S2 in the Supporting Information).

The effects on coccolith morphology following cytoskeletal disruption were reflected in the percentage of intact coccospheres present during SEM analysis. While control cells displayed 98.1 ± 0.9% intact coccospheres, only 88.3 ± 5.9% of coccospheres were intact after treatment with 1.25 μM vinblastine and only 31.1 ± 1.2% after treatment with 2 μM cytochalasin B (n = 3, ± SDl Fig. 3, a and b). Since minor malformations by definition do not affect the double shield architecture that is instrumental in forming an interlocking coccosphere, coccoliths displaying minor malformations are still able to integrate normally into the coccosphere. Coccoliths displaying major malformations, by contrast, do not interlock and therefore make the coccosphere unstable. This is reflected in the correlation between intact coccospheres and major malformations (Fig. 3c). The dependence of intact coccospheres on coccolith morphology was also observed in *Calcidiscus leptoporus* but was not quantified (Langer et al. 2006, Langer and Bode 2011). The relationship between coccolith morphology and coccosphere integrity highlights the importance of coccolith morphogenesis in coccolithophore ecology and evolution. The significance of an intact coccosphere has at least two aspects. First, an interlocking coccosphere has remarkable mechanical properties (Jaya et al. 2016) which will be impaired by heavily malformed coccoliths. Second, *Coccolithus braarudii* cannot grow without a coccosphere (Walker et al. 2018).

Effects of cytoskeletal inhibitors on Scyphosphaera apsteinii. We grew *Scyphosphaera apsteinii* in the presence of the microtubule inhibitors vinblastine and colchicine, and the actin inhibitor cytochalasin B. Treatment with 1.25 μM vinblastine and 20 μM colchicine for reduced the growth rate by 39% and 57%, respectively (Fig. 4). Treatment with 1 μM cytochalasin B for ca 20 days reduced the growth rate by 35%. The inhibitor concentrations used to cause a moderate reduction in growth rate in *S. apsteinii* are therefore similar to those in *Coccolithus braarudii*. However, these concentrations are much lower than those applied to disrupt coccolith morphology in *Emiliana huxleyi* (Langer et al. 2010), which may point to differences between species in the types of actin and microtubules (Thompson et al. 1984, Gunning et al. 2015, Howes et al. 2018) or in the uptake of the inhibitors.

The cytoskeleton inhibitors also had pronounced effects on coccolith morphology in *Scyphosphaera*

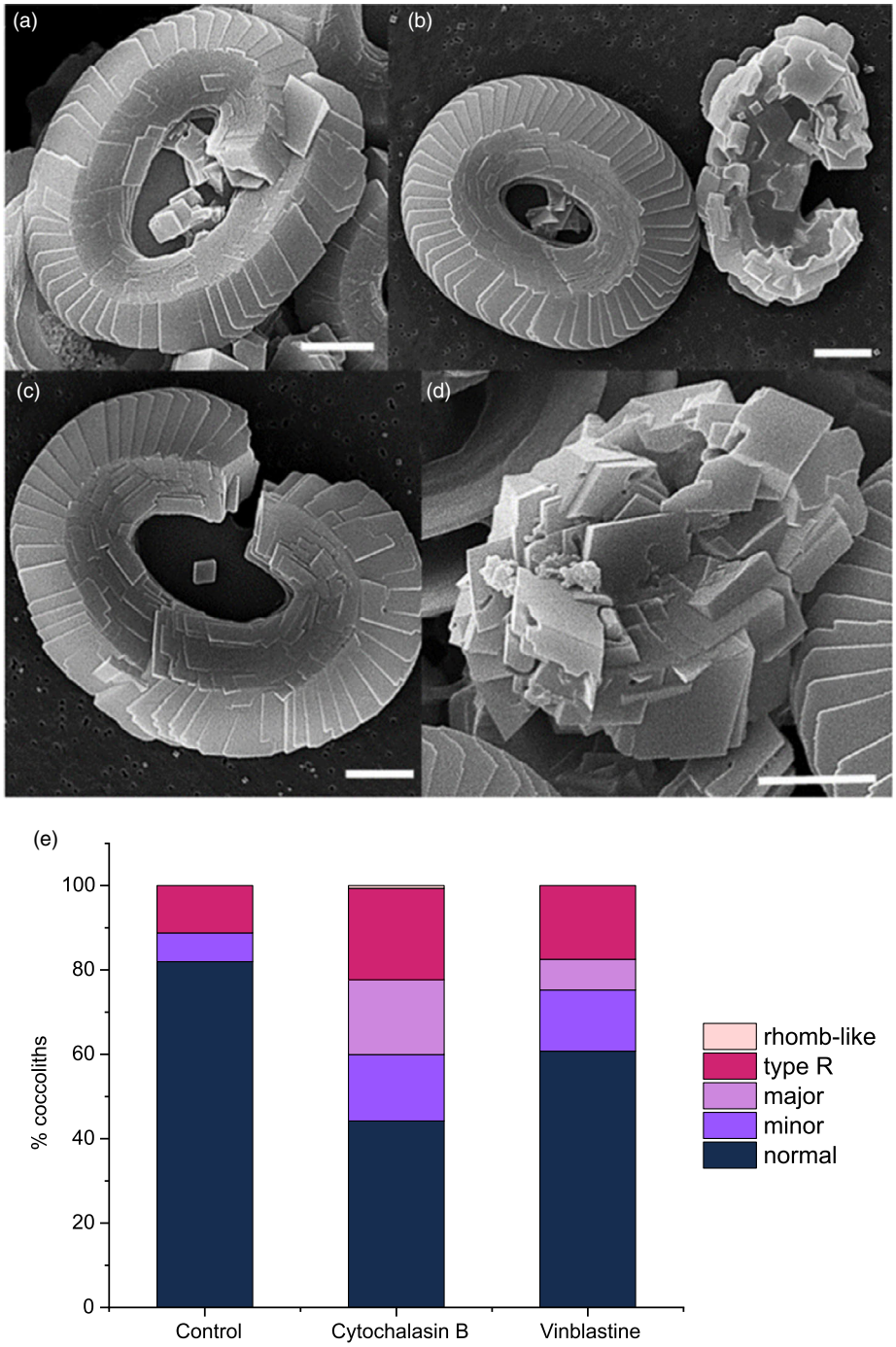

FIG. 2. Scanning electron micrographs of the morphological categories of *Coccolithus braarudii* coccoliths. Representative SEM images of the categories used to quantify coccolith morphology. (a) minor malformation, shields largely intact but elements imperfect, (b) normal coccolith (left) and major malformation (right) where shields are not correctly formed. (c) type R, coccolith largely intact but the shields do not form a complete ring (d) rhomb-like malformation, shields are not discernible, composed of 'blocky' calcite crystals. Scale bars = 2 μm. (e) Quantification of coccolith morphology. Bars from bottom up represent the morphological categories (% of counted): normal, minor malformation, major malformation, type R, and rhomb-like malformation. A minimum of 300 coccoliths were assessed for each sample, with values representing means of triplicate treatments. [Color figure can be viewed at wileyonlinelibrary.com]

apsteinii. We did not quantify the effects of cytoskeletal disruption on murolith morphology, although a qualitative analysis indicated that murolith malformations increased under all tested inhibitors (Fig. S1 in the Supporting Information). Quantitative analysis of lopadolith morphology revealed a similar morphological response to all tested inhibitors (Fig. 5). The proportion of type S,

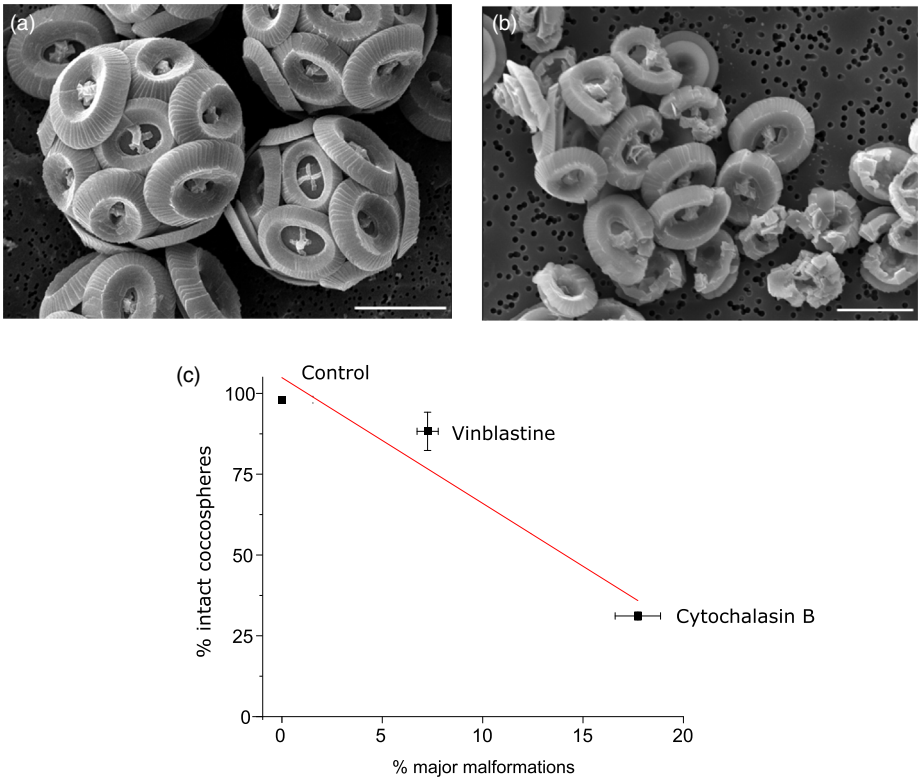

FIG. 3. Effect of coccolith malformations on the *Coccolithus braarudii* coccosphere. (a) SEM image of control cells showing intact coccospheres. Bar = 10 μm. (b) SEM image from cells treated with 2 μM cytochalasin B showing collapsed coccospheres. Bar = 10 μm. (c) Percentage of intact *C. braarudii* coccospheres versus percentage of major malformations in coccoliths. An increase in the proportion of major malformations correlates with a decrease in the % of intact coccospheres. Data points represent different treatments (control, vinblastine, and cytochalasin B). The trendline represents linear regression with an r^2 of 0.92. n = 3 replicate treatments. Error bars represent SD. [Color figure can be viewed at wileyonlinelibrary.com]

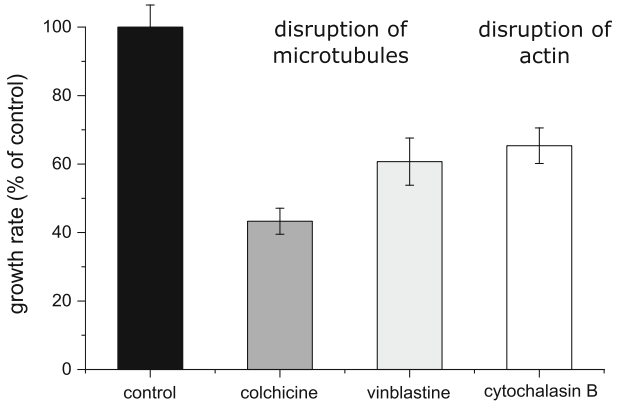

FIG. 4. Effects of cytoskeletal inhibitors on growth of *Scyphosphaera apsteinii*. Specific growth rate of *S. apsteinii* (shown relative to the control) following treatment with 20 μM colchicine, 1.25 μM vinblastine, or 1 μM cytochalasin B. n = 3 cultures for each treatment. Error bars represent SD.

type T, and type R malformations increased in under all treatments, with the proportion of normal coccoliths decreasing from 87% in control cultures to 36–54% in the presence of cytoskeleton inhibitors. As the nature of the malformations is similar between all treatments, we conclude that disruption of either the microtubule or actin networks has similar effects on coccolith morphology. It is interesting nonetheless that the treatment that had the greatest impact on growth (colchicine) did not have the greatest impact on morphology (cytochalasin B).

The coccoliths of *Scyphosphaera apsteinii* do not interlock, unlike those observed on *Coccolithus braarudii* and *Emiliana huxleyi*, and so do not usually remain intact during sample preparation for SEM analysis. We therefore did not quantify collapsed coccospheres.

DISCUSSION

Our results suggest that both microtubules and actin filaments are involved in coccolith morphogenesis in *Coccolithus braarudii* and *Scyphosphaera apsteinii*, in support of previous findings in *Emiliana huxleyi* (Langer et al. 2010). Unlike the application of the silicon analogue germanium, which results in distinct types of malformed coccoliths in *C. braarudii* and *S. apsteinii* (Langer et al. 2021), the malformations induced by disruption of the cytoskeleton were not specific to this stress (Giraudeau et al. 1993,

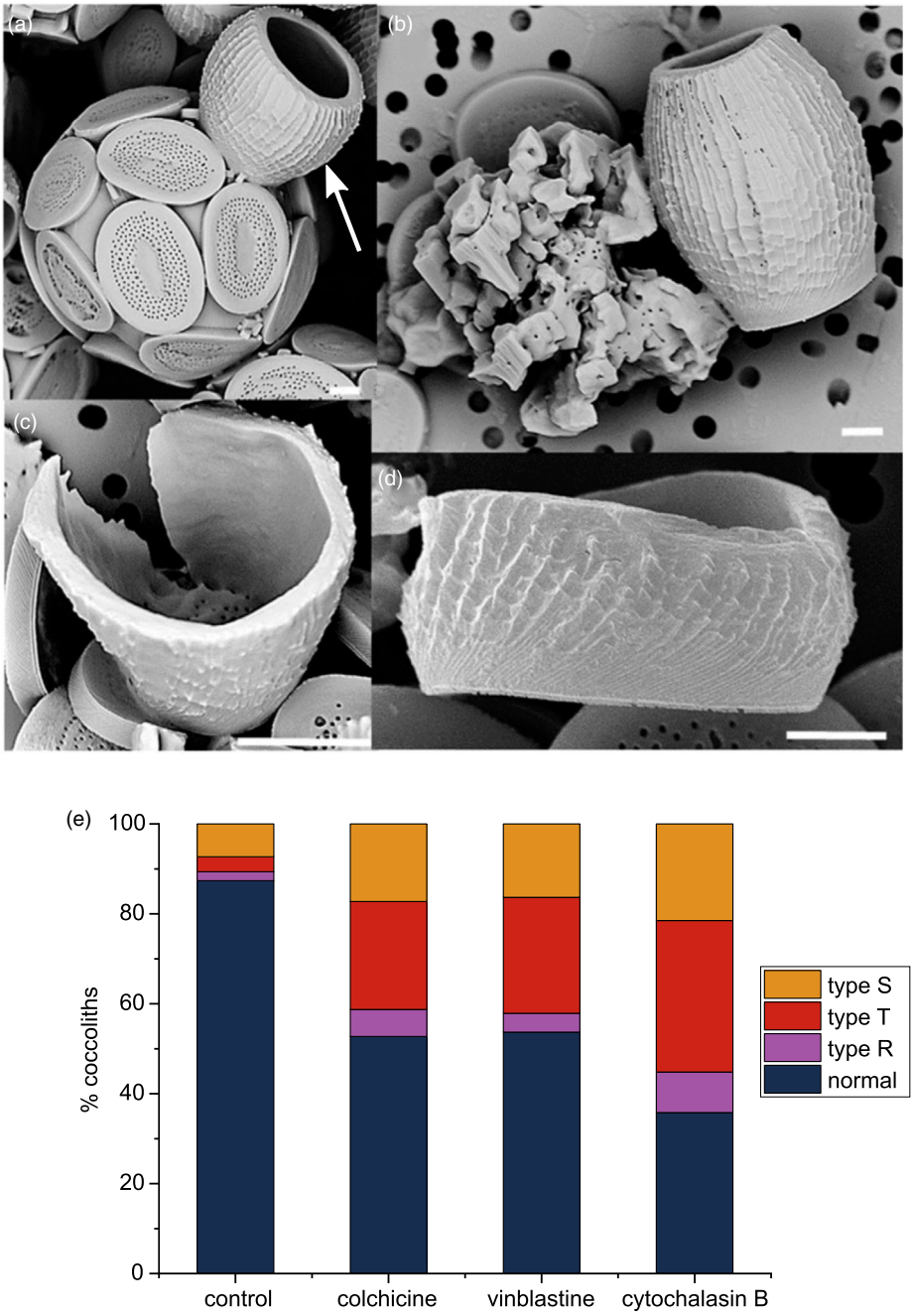

FIG. 5. Scanning electron micrographs of the morphological categories of *Scyphosphaera apsteinii* coccoliths. Representative SEM images of the categories used to quantify coccolith morphology. (a) Intact coccosphere with disc-like muroliths and barrel-shaped lopadolith (arrowed) exhibiting normal morphology, (b) type T (heavily malformed, loss of barrel shape) (left) and normal (right), (c) type R, lopadoliths barrel formed normally except that it does not form a closed cylinder. (d) type S, short lopadolith with no obvious teratological malformation. Coccoliths shown in b, c, and d are lopadoliths. Scale bars 2 μm in a, b, d, and 5 μm in c. (e) Quantitation of coccolith morphology in *S. apsteinii*. Bars from bottom up represent the morphological categories (% of counted): normal, type R, type T, type S. A minimum of 300 coccoliths were assessed for each sample, with values representing means of triplicate treatments. [Color figure can be viewed at wileyonlinelibrary.com]

Langer et al. 2006, Gerecht et al. 2015). Although cytoskeletal inhibitors did not cause specific malformations (i.e., the nature of the malformations was not uniquely linked to a specific treatment), the effects on coccolith morphogenesis are unlikely to be simply a result of general cellular stress imposed by a reduction in growth rate. Disruption of coccolith formation did not simply correlate with inhibition of growth, as treatments that gave the greatest inhibition of growth (e.g., colchicine to *C. braarudii*) did not result in the highest degree of coccolith malformations. This also supports observations from

E. huxleyi that growth inhibition via other mechanisms, such as the inhibition of photosynthesis, does not result in an increase in coccolith malformations (Langer et al. 2010). We therefore propose that the malformations we observe point to a requirement for both actin and microtubules in shaping the developing coccolith.

Disruption of actin networks with cytochalasin B in *Coccolithus braarudii* or *Scyphosphaera apsteinii* did not have a distinct effect on coccolith morphology from the disruption of microtubules with either colchicine or vinblastine, suggesting that both components of the cytoskeleton contribute to similar aspects of coccolithogenesis. This finding differs from an earlier study where disruption of actin with latrunculin B in *C. braarudii* inhibited coccolith secretion, suggesting a specific role for actin in this process (Durak et al. 2017). There are several explanations for these differing results. The phenotypic difference may simply reflect a difference in the effective concentration of the inhibitor applied, as it is difficult to gauge the extent to which the actin network has been disrupted in the two studies. The differing phenotypes may also result from the differences in the mode of action of latrunculin B and cytochalasin B. While the latrunculin B depolymerizes actin, cytochalasin B caps actin filaments thereby reducing polymerization rate (Maclean-Fletcher and Pollard 1980, Forscher and Smith 1988, Gibbon et al. 1999, Foissner and Wasteneys 2007). Differences in the experimental protocols may also have contributed to the different phenotypes. While the current study observed coccolith production over several generations, Durak et al. (2017) observed production of new coccoliths 24 h after decalcification. While this has the advantage of ensuring that only coccoliths produced following the application of the treatment are observed, the process of decalcification itself may induce malformations (Fig. S2 in the Supporting Information).

Durak et al. (2017) observed only a few heavily malformed coccoliths in SEM samples from *Coccolithus braarudii* cultures treated with latrunculin B and hypothesized that these arose from intracellular coccoliths that had not been secreted. The nature of these malformations differs from those observed in response to cytochalasin B or in response to other stressors (Giraudeau et al. 1993, Langer et al. 2006, Gerecht et al. 2015). It is therefore possible that the decalcification process contributed to these unusual malformations. In support of this conclusion, similar malformations were also observed in recalcifying cells in response to the microtubule inhibitor nocodazole (17 μM) Durak et al. (2017), but were not seen in the current study following treatment with 2 μM vinblastine. Again, these phenotypic differences could be due to differences in the concentration of inhibitor applied or their mode of action. Both nocodazole and vinblastine stabilize microtubule ends at nanomolar concentrations but depolymerize them at micromolar concentrations (Jordan et al. 1992). A difference in their effect on coccolith morphogenesis could therefore stem from the different concentrations used. However, given the relatively high proportion of malformations in recalcifying control cells, it is likely that the unusual malformations observed in response to nocodazole are the result of a combined effect of decalcification and nocodazole (Durak et al. 2017).

Disruption of the cytoskeleton could potentially influence the calcification processes in multiple ways, from the intracellular transport of substrates to the coccolith vesicle, to the direct shaping of the coccolith vesicle and the exocytosis of the mature coccolith (Durak et al. 2017). Disruption of the morphogenetic role of the cytoskeleton implies that cytoskeleton inhibitors should cause teratological malformations, rather than incomplete growth (Young and Westbroek 1991). Incomplete coccoliths may arise if transport of substrates to the coccolith vesicle is disrupted, or if the cytoskeleton is involved in the cellular 'stop signal' that prevents further crystal growth following the formation of a fully mature coccolith. In the present study, we found little evidence for the presence of incomplete coccoliths following disruption of the cytoskeleton in *Coccolithus braarudii*. We did not quantify incomplete coccoliths in *C. braarudii* because a preliminary analysis revealed that the percentage of incomplete coccoliths in all samples was less than 1%. The presence of incomplete coccoliths in *Scyphosphaera apsteinii* is slightly more difficult to resolve because it is not entirely clear whether the S-type malformation should be classified as incomplete, malformed (in the strict teratological sense), or normal. The S-type category is a short lopadolith (i.e., the length of the barrel is reduced) with no obvious teratological malformation. While this might seem to suggest that it should count as incomplete, there are several observations from different cultures suggesting that there is a great variability in lopadolith size including S-type-size (not quantified). Given this variability, it is possible that we should consider the S-type morphology as normal, rather than a malformation. However, as the S-type morphology is more abundant in response to cytoskeletal inhibitors, it does appear to represent a genuine effect, albeit an effect on size rather than "completeness". The distinction between size and incompleteness is harder to define in *S. apsteinii* than in *E. huxleyi*, in which incomplete coccoliths can be clearly identified by the absence of a well-defined rim while complete coccoliths can exhibit different sizes (Langer et al. 2010, Rosas-Navarro et al. 2016). The example of *E. huxleyi* shows that, from a mechanistic point of view, there is a distinction between size and incompleteness. An incomplete coccolith represents a situation where crystal growth was stopped too early, so that the coccolith does not possess all the normal structural

features, that is the cellular "stop-signal" was not given correctly. This situation is therefore distinct from a normal coccolith of small size. In terms of *S. apsteinii*, this means that the increase in the S-type morphology in response to cytoskeleton inhibitors does not indicate a connection between the "stop-signal" for coccolith growth and the cytoskeleton. The absence of an increase in incomplete coccoliths in *C. braarudii* (this study) or *Emiliana huxleyi* (Langer et al. 2010) further suggests that cytoskeleton inhibitors applied in this manner do not affect the stop-signal for coccolith growth.

In summary, our findings show that both actin filaments and microtubules are involved in coccolith morphogenesis in *Coccolithus braarudii* (Coccolithales) and *Scyphosphaera apsteinii* (Zygodiscales). Taken together with previous findings in *Emiliana huxleyi* (Isochrysidales; Langer et al. 2010), this strongly suggests that these two cytoskeleton elements play a central role in coccolith morphogenesis in coccolithophores. Detailed examination of the mechanisms through which the actin and microtubules interact to influence the shape of the coccolith vesicle as the coccolith matures is now required to fully test the 'dynamic mold' hypothesis. To achieve this, novel high-resolution imaging techniques, which preserve sub-cellular features, such as cryo-FIB-SEM will likely be helpful (Kadan et al. 2021). These highly specialized electron microscopy applications are difficult and time-consuming, but the results of this study show that the effort is worthwhile. Our data suggest that the cytoskeleton is at the heart of coccolith morphogenesis.

The work was supported by an NERC award to GLW (NE/N011708/1), an NSF-GEO award to ART (1638838), and an ERC Advanced Grant to CB (ERC-ADG-670390). Electron microscopy analyses were performed at the PEMC (Plymouth University, UK). The authors declare no competing interests.

Aquilano, D., Otalora, F., Pastero, L. & Garcia-Ruiz, J. M. 2016. Three study cases of growth morphology in minerals: Halite, calcite and gypsum. *Prog. Cryst. Growth Ch.* 62:227–51.

Bach, L. T., Bauke, C., Meier, K. J. S., Riebesell, U. & Schulz, K. G. 2012. Influence of changing carbonate chemistry on morphology and weight of coccoliths formed by *Emiliania huxleyi*. *Biogeosci.* 9:3449–63.

Baumann, K. H., Bockel, B. & Frenz, M. 2004. Coccolith contribution to south Atlantic carbonate sedimentation. *In* Thierstein, H. R. & Young, J. R. [Eds.] *Coccolithophores: from molecular processes to global impact*. Springer, Berlin, pp. 367–402.

Bown, P. R., Lees, J. A. & Young, J. R. 2004. Calcareous nannoplankton evolution and diversity through time. *In* Thierstein, H. R. & Young, J. R. [Eds.] *Coccolithophores: from molecular processes to global impact*. Springer, Berlin, pp. 481–508.

Daniels, C. J., Poulton, A. J., Young, J. R., Esposito, M., Humphreys, M. P., Ribas-Ribas, M., Tynan, E. & Tyrrell, T. 2016. Species-specific calcite production reveals *Coccolithus pelagicus* as the key calcifier in the Arctic Ocean. *Mar. Ecol. Prog. Ser.* 555:29–47.

Didymus, J. M., Young, J. R. & Mann, S. 1994. Construction and morphogenesis of the chiral ultrastructure of coccoliths from the marine alga *Emiliania huxleyi*. *P. R. Soc. B* 258:237–45.

Dixon, H. H. 1900. On the structure of coccospheres and the origin of coccoliths. *Proc. R. Soc. Lond.* 66:305–15.

Drescher, B., Dillaman, R. M. & Taylor, A. R. 2012. Coccolithogenesis in *Scyphosphaera apsteinii* (Prymnesiophyceae). *J. Phycol.* 48:1343–61.

Durak, G. M., Brownlee, C. & Wheeler, G. L. 2017. The role of the cytoskeleton in biomineralisation in haptophyte algae. *Sci. Rep.* 7:15409.

Foissner, I. & Wasteneys, G. O. 2007. Wide-ranging effects of eight cytochalasins and latrunculin A and B on intracellular motility and Actin filament reorganization in characean internodal cells. *Plant Cell Phys.* 48:585–97.

Forscher, P. & Smith, S. J. 1988. Actions of cytochalasins on the organization of Actin-filaments and microtubules in a neuronal growth cone. *J. Cell Biol.* 107:1505–16.

Freud, S. 1882. Ueber den bau der nervenfasern und nervenzellen beim flusskrebs. sitzungsber. *Akad. Wien Math-Naturwiss Classe* 85:9–46.

Gerecht, A. C., Supraha, L., Edvardsen, B., Langer, G. & Henderiks, J. 2015. Phosphorus availability modifies carbon production in *Coccolithus pelagicus* (Haptophyta). *J. Exp. Mar. Biol. Ecol.* 472:24–31.

Gibbon, B. C., Kovar, D. R. & Staiger, C. J. 1999. Latrunculin B has different effects on pollen germination and tube growth. *Plant Cell* 11:2349–63.

Giraudeau, J., Monteiro, P. M. S. & Nikodemus, K. 1993. Distribution and malformation of living coccolithophores in the northern Benguela upwelling system off Namibia. *Mar. Micropaleontol.* 22:93–110.

Guillard, R. R. L. 1975. Culture of phytoplankton for feeding marine invertebrates. *In* Smith, W. L. & Chanley, M. H. [Eds.] *Culture of Marine Invertebrate Animals*. Plenum Press, New York, pp. 29–60.

Gunning, P. W., Ghoshdastider, U., Whitaker, S., Popp, D. & Robinson, R. C. 2015. The evolution of compositionally and functionally distinct Actin filaments. *J. Cell Sci.* 128:2009–19.

Henriksen, K., Stipp, S. L. S., Young, J. R. & Bown, P. R. 2003. Tailoring calcite: nanoscale AFM of coccolith biocrystals. *Am. Mineral.* 88:2040–4.

Henriksen, K., Stipp, S. L. S., Young, J. R. & Marsh, M. E. 2004. Biological control on calcite crystallization: AFM investigation of coccolith polysaccharide function. *Am. Mineral.* 89:1709–16.

Howes, S. C., Geyer, E. A., LaFrance, B., Zhang, R., Kellogg, E. H., Westermann, S., Rice, L. M. & Nogales, E. 2018. Structural and functional differences between porcine brain and budding yeast microtubules. *Cell Cycle* 17:278–87.

Huxley, T. H. 1868. On some organisms living at great depth in the North Atlantic Ocean. *Quart. J. Microscop. Sci.* 8:203–12.

Jaya, B. N., Hoffmann, R., Kirchlechner, C., Dehm, G., Schen, C. & Langer, G. 2016. Coccospheres confer mechanical protection: New evidence for an old hypothesis. *Acta Biomater.* 42:258–64.

Jordan, M. A., Thrower, D. & Wilson, L. 1992. Effects of vinblastine, podophyllotoxin and nocodazole on mitotic spindles - implications for the role of microtubule dynamics in mitosis. *J. Cell Sci.* 102:401–16.

Kadan, Y., Tollervey, F., Varsano, N., Mahamid, J. & Gal, A. 2021. Intracellular nanoscale architecture as a master regulator of calcium carbonate crystallization in marine microalgae. *Proc. Natl. Acad. Sci. USA* 118:e2025670118.

Klaveness, D. 1972. *Coccolithus huxleyi* (Lohmann) Kamptner. I. Morphologic investigations on the vegetative cell and the process of coccolith formation. *Protistologica* 8:335–46.

Klaveness, D. 1976. *Emiliania huxleyi* (Lohmann) Hay and Mohler. 3. Mineral deposition and origin of matrix during coccolith formation. *Protist* 12:217–24.

Langer, G. & Benner, I. 2009. Effect of elevated nitrate concentration on calcification in *Emiliania huxleyi*. *J. Nannoplankton Res.* 30:77–80.

Langer, G. & Bode, M. 2011. CO_2 mediation of adverse effects of seawater acidification in *Calcidiscus leptoporus*. *Geochem. Geophy. Geosyst.* 12:Q05001.

Langer, G., de Nooijer, L. J. & Oetjen, K. 2010. On the role of the cytoskeleton in coccolith morphogenesis: the effect of cytoskeleton inhibitors. *J. Phycol.* 46:1252–6.

Langer, G., Geisen, M., Baumann, K. H., Klas, J., Riebesell, U., Thoms, S. & Young, J. R. 2006. Species-specific responses of calcifying algae to changing seawater carbonate chemistry. *Geochem. Geophy. Geosyst.* 7:Q09006.

Langer, G., Oetjen, K. & Brenneis, T. 2012. Calcification of *Calcidiscus leptoporus* under nitrogen and phosphorus limitation. *J. Exp. Mar. Biol. Ecol.* 413:131–7.

Langer, G., Oetjen, K. & Brenneis, T. 2013. On culture artefacts in coccolith morphology. *Helgoland Mar. Res.* 67:359–69.

Langer, G., Taylor, A. R., Walker, C. E., Meyer, E. M., Ben Joseph, O., Gal, A., Harper, G. M., Probert, I., Brownlee, C. & Wheeler, G. L. 2021. Role of silicon in the development of complex crystal shapes in coccolithophores. *New Phytol.* 231:1845–57.

Maclean-Fletcher, S. & Pollard, T. D. 1980. Mechanism of action of cytochalasin-B on Actin. *Cell* 20:329–41.

Marsh, M. E. 1994. Polyanion-Mediated Mineralization - Assembly and reorganization of acidic polysaccharides in the golgi system of a coccolithophorid alga during mineral deposition. *Protoplasma* 177:108–22.

Marsh, M. E. 1999. Coccolith crystals of *Pleurochrysis carterae*: crystallographic faces, organization, and development. *Protoplasma* 207:54–66.

Marsh, M. E., Ridall, A. L., Azadi, P. & Duke, P. J. 2002. Galacturonomannan and Golgi-derived membrane linked to growth and shaping of biogenic calcite. *J. Struct. Biol.* 139:39–45.

Monteiro, F. M., Bach, L. T., Brownlee, C., Bown, P., Rickaby, R. E., Poulton, A. J., Tyrrell, T. et al. 2016. Why marine phytoplankton calcify. *Sci. Adv.* 2:e1501822.

Outka, D. E. & Williams, D. C. 1971. Sequential coccolith morphogenesis in *Hymenomonas-carterae*. *J. Protozool.* 18:285–97.

Poulton, A. J., Adey, T. R., Balch, W. M. & Holligan, P. M. 2007. Relating coccolithophore calcification rates to phytoplankton community dynamics: Regional differences and implications for carbon export. *Deep-Sea Res Pt Ii* 54:538–57.

Probert, I., Fresnel, J., Billard, C., Geisen, M. & Young, J. R. 2007. Light and electron microscope observations of *Algirosphaera robusta* (Prymnesiophyceae). *J. Phycol.* 43:319–32.

Quintero-Torres, R., Arago, J. L., Torres, M., Estrada, M. & Cros, L. 2006. Strong far-field coherent scattering of ultraviolet radiation by holococcolithophores. *Phys. Rev. E* 74:032901.

Remak, R. 1843. Ueber den inhalt der nervenprimitivroehren. *Müllers Archiv.* 8:197–201.

Rosas-Navarro, A., Langer, G. & Ziveri, P. 2016. Temperature affects the morphology and calcification of *Emiliania huxleyi* strains. *Biogeosci.* 13:2913–26.

Taylor, A. R. & Brownlee, C. 2003. A novel Cl^- inward-rectifying current in the plasma membrane of the calcifying marine phytoplankton *Coccolithus pelagicus*. *Plant Physiol.* 131:1391–400.

Taylor, A. R., Russell, M. A., Harper, G. M., Collins, T. F. T. & Brownlee, C. 2007. Dynamics of formation and secretion of heterococcoliths by *Coccolithus pelagicus* ssp *braarudii*. *Eur. J. Phycol.* 42:125–36.

Thompson, W. C., Asai, D. J. & Carney, D. H. 1984. Heterogeneity among microtubules of the cytoplasmic microtubule complex detected by a monoclonal-antibody to alpha tubulin. *J. Cell Biol.* 98:1017–25.

Walker, C. E., Taylor, A. R., Langer, G., Durak, G. M., Heath, S., Probert, I., Tyrrell, T., Brownlee, C. & Wheeler, G. L. 2018. The requirement for calcification differs between ecologically important coccolithophore species. *New Phytol.* 220:147–62.

Westbroek, P., Dejong, E. W., Vanderwal, P., Borman, A. H., Devrind, J. P. M., Kok, D., Debruijn, W. C. & Parker, S. B. 1984. Mechanism of calcification in the marine alga *Emiliania huxleyi*. *Phil. Trans. Roy. Soc. B Biol. Sci* 304:435.

Wilbur, K. M. & Watabe, N. 1963. Experimental studies on calcification in molluscs and the alga *Coccolithus huxleyi*. *Ann. NY Acad. Sci.* 109:82–112.

Young, J. R. 1994. Functions of coccoliths. *In* Winter, A. & Siesser, W. G. [Eds.] *Coccolithophores*. Cambridge University Press, Cambridge, UK, pp. 63–82.

Young, J. R., Andruleit, H. & Probert, I. 2009. Coccolith function and morphogenesis: insights from appendage-bearing coccolithophores of the family Syracosphaeraceae (Haptophyta). *J. Phycol.* 45:213–26.

Young, J. R., Davis, S. A., Bown, P. R. & Mann, S. 1999. Coccolith ultrastructure and biomineralisation. *J. Struct. Biol.* 126:195–215.

Young, J. R. & Westbroek, P. 1991. Genotypic variation in the coccolithophorid species *Emiliania huxleyi*. *Mar. Micropaleontol.* 18:5–23.

Ziveri, P., de Bernardi, B., Baumann, K. H., Stoll, H. M. & Mortyn, P. G. 2007. Sinking of coccolith carbonate and potential contribution to organic carbon ballasting in the deep ocean. *Deep Sea Res. II* 54:659–75.

Supporting Information

Additional Supporting Information may be found in the online version of this article at the publisher's web site:

Figure S1. Cytoskeleton inhibitors also induce malformations in *Scyphosphaera apsteinii* muroliths. In addition to barrel-shaped lopadoliths, *S. apsteinii* also produces disc-like muroliths (Fig. 5). Muroliths also exhibited distinct malformations in cells treated with cytoskeleton inhibitors, although these were not quantified. The SEM image shown illustrates malformed muroliths from a *S. apsteinii* cell treated with 1 μM cytochalasin B. Bar = 4 μm.

Figure S2. Coccolith malformations due to decalcification treatments. Bright-field images of recalcification in *Coccolithus braarudii* after decalcification with either EGTA (Taylor and Brownlee 2003; left column) or low pH (rapid acidification followed by buffering; right column). (a, b) Cells immediately after decalcification (0 h). (c, d) 4 h after decalcification. (e, f) 8 h after decalcification. (g, h) 24 h after decalcification. The images show that after the initial decalcification (0 h), a mature internal coccolith was observed inside cells. After 4 h incubation in fresh media, cells typically had either secreted the mature internal coccolith or produced a malformed coccolith (arrows). At least one or two coccoliths produced by each cell show substantial malformations after either of the acute decalcification treatments. Cells are able to be fully recalcify over 24–48 h. Scale bars = 10 μm.

Table S1. Summary of cytoskeleton inhibitors used to disrupt coccolithophore calcification.

Table S2. Definitions of the different categories for coccolith morphologies.